Structures xxx (2016) xxx–xxx

Contents lists available at ScienceDirect

Structures

journal homepage: www.elsevier.com/locate/structures

Axial Compression Behaviour of Long Concrete Filled Double Skinned Steel Tubular Columns

Sulthana U. M., Jayachandran S. A. *

Department of Civil Engineering, Indian Institute of Technology Madras, Chennai, India

ARTICLE INFO

Article history:
Received 8 May 2016
Received in revised form 21 October 2016
Accepted 7 December 2016
Available online xxxx

Keywords:
CFDST
Long columns
Confinement effect
Global buckling
Axial capacity
Reduction factors

ABSTRACT

Concrete filled double skinned steel tubes (CFDST) are proved to have good structural performance in terms of strength, stiffness, ductility and fire resistance. Long CFSDT columns find application in elevated corridors, bridge piers and also in buildings. However, the behaviour of CFDST long columns is still not fully understood and there is limited research in this area. In this paper, axial capacity equations for long column CFDST sections are proposed based on strength super-position method of design. Column capacity computed using the proposed equation is validated through experimental studies conducted by the authors (for columns having L/D ratio of 20) as well as additional tests reported in literature. Tests were conducted on CFDST, Concrete Filled Steel Tube (CFST) and Concrete Filled Hollow Single skinned Steel Tube (CFHSST) cross-sections. Parameters considered in the test include (i) length of the column, (ii) shape of the inner tube, and (iii) absence of inner tube. Results from the test viz., (a) load carrying capacity, (b) load vs. axial deformation curves, and (c) load vs. lateral deflection curves, have been reported. Test result shows that the contribution of inner tube on the axial capacity of long column is less than the predicted value, as the column undergoes elastic buckling prior to yielding. A reduction factor is proposed to account for the reduced contribution of inner steel tube, and it is applied as a correction to the initially proposed equations. The results from proposed capacity equation are compared with experimental results and are found to be in good agreement. It is concluded that the long column axial capacity equation specified for CFST in AISC-360 and EC4 could be extended for CFDST sections after incorporating the new reduction factor.

1. Introduction

The concept of CFDST was first introduced in underwater pressure vessels [1], where the high bending stiffness of the cross-section was utilized to prevent instability under external pressure. It is also applicable for nuclear, liquid and gas containment, and blast resistant shelters [1]. Owing to its good damping and energy absorption properties and light weight cross-sections, CFDST was used as tall piers for bridges in Japan [2]. Further, CFDST columns have been used in electric transmission towers in China [3]. They are predicted to perform well under blast load [4], impact load [5] and in the instance of fire, they show better structural response due to the presence of concrete encased inner tube [6]. The inner steel tube also plays an important role in mitigating a rupture failure when ultra-high strength materials are used [7]. A state-of-art report on development and advanced applications of concrete filled steel tubular structures is reported by Han et al. (2014) [8].

Studies were carried out on CFDST stub columns having $L/D < 5$, [2,9,10,11]. However, studies to ascertain the behaviour of long column CFDST is limited. Mechanics based model was developed by Han et al. (2009) [12], to predict the beam-column behaviour of CFDST section under axial and cyclic loading and design formulae for CFDST columns and beam-columns were suggested. Tapered CFDST long columns were studied experimentally and numerically Li et al. (2013) [13], and an equation to predict the elastic buckling capacity of tapered CFDST long column is recommended. Finite Element Analysis (FEA) model was developed in ABAQUS to study the preload effect on steel tubes in CFDST column and design formulae were proposed to estimate the reduced axial strength of CFDST with preloads [14]. It was observed that the column slenderness has the highest significance on CFDST column

Abbreviations: A_c, area of in-filled concrete; A_s, area of steel tube; A_{si}, A_{so}, area of inner and outer steel tubes respectively; D, diameter of CFST specimen; D_h, diameter of hollow core; D_i, D_o, diameter of inner and outer steel tubes respectively; E_c, modulus of elasticity of concrete; E_s, modulus of elasticity of steel; E_{si}, E_{so}, modulus of elasticity of inner and outer steel tubes respectively; EI_{eff}, effective flexural rigidity; f_{yi}, f_{yo}, yield strength of inner and outer steel tubes respectively; f_{ck}, 28-day mean cube strength of in-filled concrete; f'_c, cylinder compressive strength of in-filled concrete; I_c, moment of inertia of concrete section about the elastic neutral axis of the composite section; I_s, moment of inertia of steel shape about the elastic neutral axis of the composite section; I_{si}, moment of inertia of inner steel tube about the elastic neutral axis of the composite section; I_{so}, moment of inertia of outer steel tube about the elastic neutral axis of the composite section; L, length of the test specimen; P_n, nominal axial strength of zero length; $P_{u,n}$, nominal axial strength; P_{cr}, elastic critical buckling load; t_o, thickness of outer steel tube; t_i, thickness of inner steel tube.

* Corresponding author.
E-mail address: aruls@iitm.ac.in (J. S. A.).

http://dx.doi.org/10.1016/j.istruc.2016.12.002
2352-0124/

strength index. Even though, long column range is covered in the above studies, the parameters considered are on diverse features like, tapered section, eccentric loading, preloads etc.

Comprehensive studies on long column CFDST under pure axial loads is found in very few experimental works [15] and [16]. Circular Hollow Section (CHS) in CHS cross-section is considered in both studies. Steel sections with yield strengths ranging from 319 MPa to 549 MPa and concrete with compressive strengths ranging from 28 MPa to 33 MPa was used by Essopjee and Dundu (2015) [15], for L/D ratio in the range of 5 to 18. In Romero et al. (2015) [17], normal strength steel (yield strength ranging from 272 MPa to 414 MPa) and a combination of normal strength concrete (30 MPa) and ultra-high strength concrete (150 MPa) was used for experiment with column L/D ratio of 16.575. It was found that the axial capacity predicted using the equations specified in EC4 [18] for CFST (modified and applied for CFDST), is un-conservative. While it is said in stub column research that the column design equations of CFST section could be extended for CFDST sections, it is not applicable for long column CFDST sections. More studies are needed to develop a robust design procedure for long column CFDST.

In the present study, long column CFDST with square cross-section is selected for experiments as there is little published work on this cross-sectional configuration. The accuracy of the predicted axial capacities using available design procedures for CFDST columns is validated by comparing with the experimental results in the present work and from the available literature.

2. Experimental program

A total of five specimens with L/D ratio of 20 are selected for this experimental study. All five specimens have unique cross-sections (Fig. 1). The specimens include one CFST section which is treated as a benchmark specimen in this study. Two CFDST and two CFHSST cross-sections are considered for the test. The outer tube is a SHS section and its dimensions are kept constant in all the specimens. Two different shapes (square and circular) are selected for the inner tube in CFDST, to understand its shape effect in the long column range. In CFHSST sections also, circular and square type hollow shapes are made for a comparative study with CFDST sections.

2.1. Geometric and material properties of test specimens

Hot rolled steel tubes supplied by TATA Steel were used for both inner and outer tubes. The steel tubes were rolled and supplied in a single batch and therefore one set of tension coupon test was sufficient for verifying the yield strength. Material characterization was carried out based on IS:1608-2005 and the average yield strength of the steel tube was found as 357.9 N/mm^2. The steel tubes were measured for straightness before commencing the experimental process and the global imperfections were well within the tolerance limit of $L/1000$. The cross-section dimensions of the steel tubes are presented in Table 1. Here, the specimens are identified in three terms. The first term refers to number of steel tubes in the cross-section; SS – single skin; DS – double skin and HSS – hollow single skin. Second term refers to shape of the steel tubes in the order of outer first and inner next; S – square and C – circular. Third term gives the length to width ratio (L/D) of the column. A constant value of 0.35 was considered as the hollowness ratio (defined as the ratio of inner diameter to outer diameter of the sandwiched concrete core) of the CFDST section.

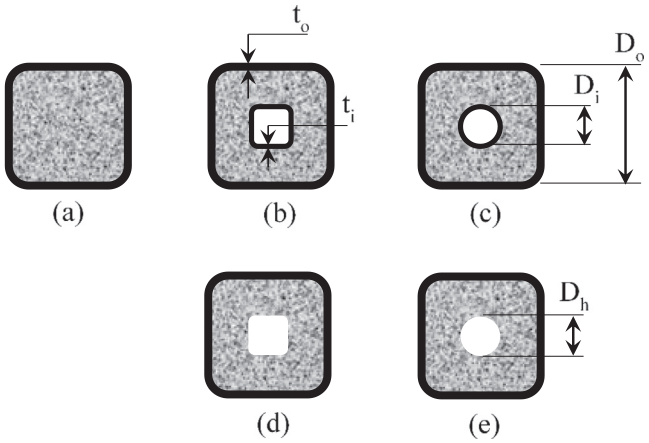

Fig. 1. Cross-section details of test specimens.

Normal strength concrete is chosen as the infill material for all the test specimens. Concrete cubes of size 150 mm × 150 mm × 150 mm were cast, compacted, cured and tested as per IS:516-1959 in UTM. The average 28-day strength of concrete was found to be 38.8 N/mm^2.

2.2. Specimen preparation

The steel tubes were supplied in a standard length of 4.5 m, later they were cut and the edges were milled for a required length of 3.6 m. Steel tubes were weld to a 12 mm thick base plate on one end and the other end was left free to facilitate concreting. In CFDST, the uniformity in the gap between the inner and outer tubes is maintained by tig welding a spacer bar between the tubes at the free end of the specimen. Concrete was poured, while the specimen was kept inclined at an angle of 45° to the ground to reduce the free fall height of concrete, in order to avoid segregation. In CFDST and CFHSST, the inner tube was kept closed at the concreting end to avoid accidental concrete intrusion in the hollow region which is undesirable for the study. In CFHSST, the inner tube is provided with a hook so that it could be removed using a crane just after the setting of concrete to form an unreinforced inner concrete edge. The specimens were allowed to cure in upright position under room temperature for 28 days. Before setting the specimen in the loading frame, the specimen ends are prepared. The excess concrete in the free edge was chipped off and milled smooth. The outer tube was weld to a 12 mm thick plate to develop uniform transfer of load across the cross-section while loading. The specimen was painted white and gridlines were marked to aid for a visual inspection of deformations while loading.

2.3. Test set-up, instrumentation and loading

The specimens were tested under axial compression load in the Structural Engineering Laboratory, at IIT Madras. The specimen was held in a loading frame of 600 T capacity (Fig. 2) with pinned-pinned boundary condition, which is ensured by ball and socket type of end-plates. These end-plates are sufficiently hardened such that they transfer load to the specimen without undergoing deformation in itself. The verticality of the specimen was checked using laser beam and spirit level. The specimen was loaded from the bottom end through a hydraulic jack of 500 T capacity. A schematic diagram of test set-up is shown in Fig. 3.

Table 1
Material and geometric properties of test specimens.

Specimen ID	Diameter and thickness				Material properties		
	D_o (mm)	t_o (mm)	D_i/D_h (mm)	t_i (mm)	f_{yo} (N/mm^2)	f_{yi} (N/mm^2)	f_{ck} (N/mm^2)
SS-S-20	180	5	–	–	357.9	–	38.8
DS-SS-20	180	5	60	3.2	357.9	357.9	38.8
DS-SC-20	180	5	60.3	3.6	357.9	357.9	38.8
HSS-SS-20	180	5	60	–	357.9	–	38.8
HSS-SC-20	180	5	60.3	–	357.9	–	38.8

Please cite this article as: U. M. S, S. A. J, Axial Compression Behaviour of Long Concrete Filled Double Skinned Steel Tubular Columns, Structures (2016), http://dx.doi.org/10.1016/j.istruc.2016.12.002

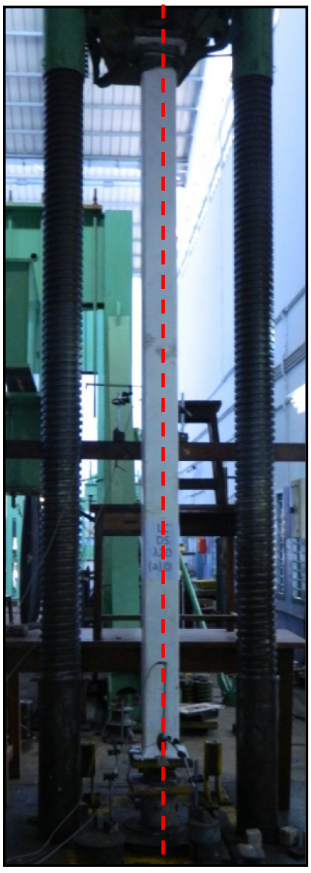

Fig. 2. Test set-up of typical specimen.

Linear Variable Displacement Transducers (LVDTs) are used for measuring the axial deformation and lateral displacement of the specimen under loading. In total, four LVDTs were used: two at the loading end and two at the mid-height to measure the axial shortening and lateral deformation respectively (Fig. 4). Strain gauges were pasted on two opposite sides at the loading end of the specimen (Fig. 4). The purpose of installing strain gauges was to ensure uniform loading across the cross-section. Axial compressive load was applied through hydraulic jack at an interval of 1/15th of the axial capacity of the specimen and each increment was sustained for a time period of 1 min. Loading was carried out till failure of specimen, which was overall buckling (sudden drop in load and rapid increase in lateral deflection) followed by yielding of cross-section. The deformations measured from LVDTs and strain gauges were saved in a data logger.

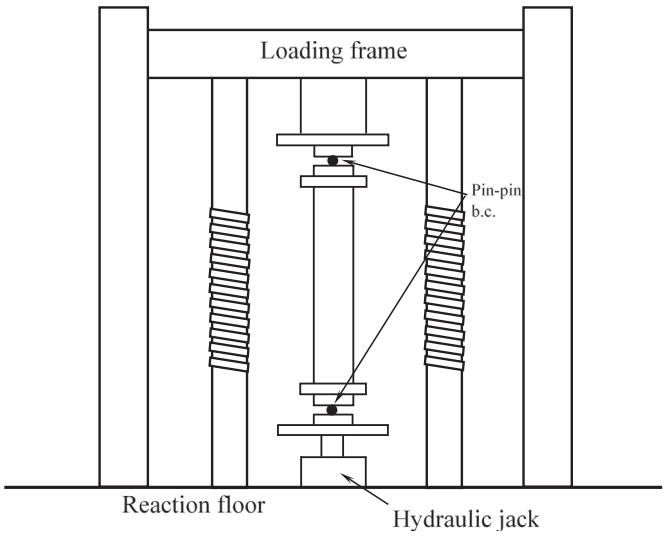

Fig. 3. Schematic diagram of test set-up.

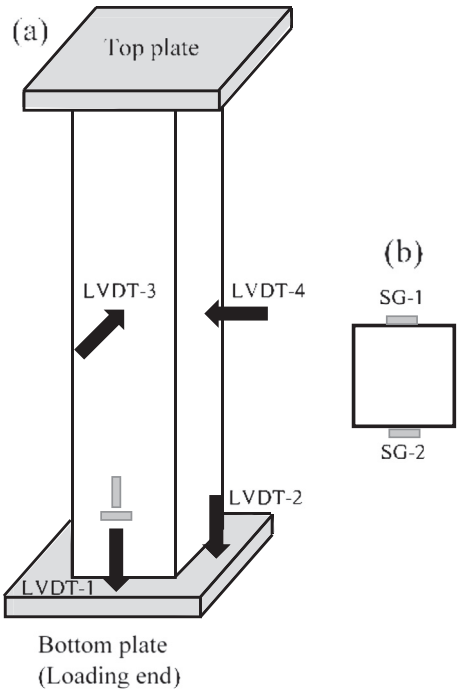

Fig. 4. Schematic diagram of instrumentation of test specimen. (a) Location of LVDTs (b) Location of strain gauges across the cross-section of specimen.

2.4. Failure pattern

The specimens failed by overall buckling followed by yielding of the cross-section, irrespective of the type of cross-section (Fig. 5). At the post-buckling phase, cross-sectional yielding occurred at the mid-height of the specimen, where a local bulge was also formed at the compression side of the outer steel tube. The yielded portion of the specimen is shown as a blow out of original photograph (Fig. 5). Overall buckling in long CFDST columns was also reported in [17] and [15].

Fig. 5. Typical failure pattern of long column specimen.

Please cite this article as: U. M. S, S. A. J, Axial Compression Behaviour of Long Concrete Filled Double Skinned Steel Tubular Columns, Structures (2016), http://dx.doi.org/10.1016/j.istruc.2016.12.002

However, the post-buckling observations of these tests are not explained in detail.

In the present study, the buckled shape of the specimen is indicated by a vertical yellow line in Fig. 5. The outer tube was cut open to study the deformation in the inner steel tube. The overall bent profile of inner tube was in coherence with the outer steel tube profile, however localized bulges were not found. It could be concluded that the inner and outer steel tubes underwent same mode of buckling due to the composite action within the cross-section. In post-buckling, the highly stressed cross-section at the mid-height of the specimen undergoes yielding. However, yielding of inner steel tube is not very evident as observed in the outer steel tube.

A strain gradient (Fig. 6) was formed within the cross-section, when the specimen underwent overall buckling. Therefore, at yielding stage, strain in outer steel tube is much higher than the strain in inner steel tube. When the extreme fibre in outer steel tube reached the yield strain, yielding was observed which led to the ultimate failure of the specimen. However, the inner steel tube did not yield, and this behaviour can be attributed to the presence of a strain gradient across the section. This has to be accounted in the design equations.

2.5. Test results

The axial load versus axial deformation in the test specimens are plotted in Fig. 7. In the linear range of the curves, the steel tubes and concrete undergo deformation at different rates due to difference in their Poisson's ratio. On further loading, micro-cracks are formed in the concrete which increases the expansion rate of concrete on par with steel tubes. At this stage, composite action is developed at the steel-concrete interface. In addition to compressive load applied from the jack, the steel tubes also experience pressure from the infill concrete. When the compressive stress in steel tube exceeds its critical buckling stress, the specimen undergoes buckling in its first Eigen mode. The behaviour of all test specimens is similar till buckling load. However, in the post-buckling range, when the cross-section of the specimen undergoes yielding, they show distinct behaviour with respect to the type of cross-section. In CFDST sections (DS-SS-20 and DS-SC-20), even though the specimen stops resisting more load after the yield of outer steel tube, it sustains the load due to the presence of inner steel tubes. This type of load sustenance is not observed in CFHSST sections (HSS-SS-20 and HSS-SC-20). Here the post-peak curves descend in a steep manner.

In the linear range (till 80% of ultimate load) of axial load versus lateral deflection curves (Fig. 8), the deflection values are very minimal, which proves that the initial global imperfections are quite small. Later, when the specimen undergoes global buckling, the lateral deflections increase drastically. The trend in load sustenance for the post-peak regime depends on the type of cross-section of the specimen. CFDST sections show ductile behaviour by withstanding axial loads for larger lateral deflections.

The axial capacity values from the test are normalized with respect to theoretical stub column capacity of the benchmark CFST specimen. The difference in the axial capacity of CFHSST and CFDST sections is very less. Increase in steel quantity for square and circular inner tube is 17% and 14% respectively when compared with CFHSST specimens. However, increase in strength of CFDST section in comparison with corresponding CFHSST is only 5% for both DS-SS-20 and DS-SC-20 specimens. This proves that for long columns, the inner tube in CFDST does not effectively contribute to the axial capacity. Normalized axial capacity and normalized axial stiffness of test specimens is shown in Figs. 9 and 10 respectively.

With regard to the shape of inner steel tubes, circular tube was expected to perform better over square tubes, as circular shape could accommodate more concrete infill compared to a square one and also, their confinement effect is higher. However, the shape had no effect as the significance of inner steel tube has reduced for long columns.

3. Design of CFDST columns

CFDST columns could be designed based on the principle of strength super position method as adopted in the case of CFST columns. It is assumed that, sections in which the inner tube is also filled with concrete (double tubes), the inner tube can be treated as reinforcement within the CFST section [19]. However, sections having hollow inner tubes are assumed as CFST, where the central part of in-filled concrete is removed and replaced with a steel tube (Fig. 11). In the CFDST stub column studies, the outer tube is observed to have more influence over the confinement of concrete, whereas the inner tube behaves more like a hollow steel tube [2,9,10,11,20]. Hence, the capacity equations proposed for the CFDST stub columns do not consider the strength of inner steel tube for the enhancement of concrete strength. In the case of long columns, concrete confinement is not significant and so it is not considered in the design, whereas, stability reduction factor governs the design. The significance of inner steel tube in the computation of stability reduction factor is yet to be explored.

The axial load capacity equation for CFDST columns is derived based on AISC-360 [21] and EC4. The design formulae of CFST columns are modified to obtain the capacity equation for CFDST columns.

3.1. AISC-360

The cross-section capacity (P_n) of CFST section in Eq. (1) is modified for CFDST section in Eq. (2). The strength due to inner tube is linearly added to the capacity equation of CFST. In CFDST, there are two possible implications in cross-section strength due to removal of concrete and replacing it with steel tube: the confinement effect can either enhance due to stiffer steel tube inclusion; or it can decrease because of hollowness of the cross-section and local buckling of inner steel tube. However, in Eq. (2), no enhancement or reduction factor is considered in computing concrete strength (i.e. it is assumed that confinement effect of concrete is unaltered when concrete core is replaced with steel tube).

$$P_n = f_{yo}A_{so} + C_2 f'_c A_c \tag{1}$$

$$P_n = f_{yo}A_{so} + f_{yi}A_{si} + C_2 f'_c A_c \tag{2}$$

The C_2 factor in Eqs. (1) and (2), is assumed such that if both outer and inner steel tubes are circular it is 0.95, otherwise it is 0.85. The member capacity ($P_{u,n}$) and the elastic buckling load (P_{cr}) of CFST is presented in Eqs. (3) and (4) respectively.

$$P_{u,n} = P_n \ 0.658^{\frac{P_n}{P_{cr}}} \tag{3}$$

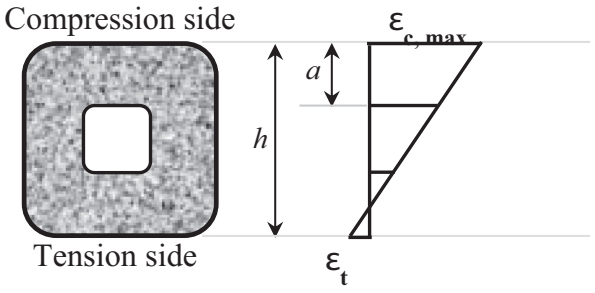

Fig. 6. Strain gradient within the yielding cross-section of CFDST column.

Please cite this article as: U. M. S, S. A. J, Axial Compression Behaviour of Long Concrete Filled Double Skinned Steel Tubular Columns, Structures (2016), http://dx.doi.org/10.1016/j.istruc.2016.12.002

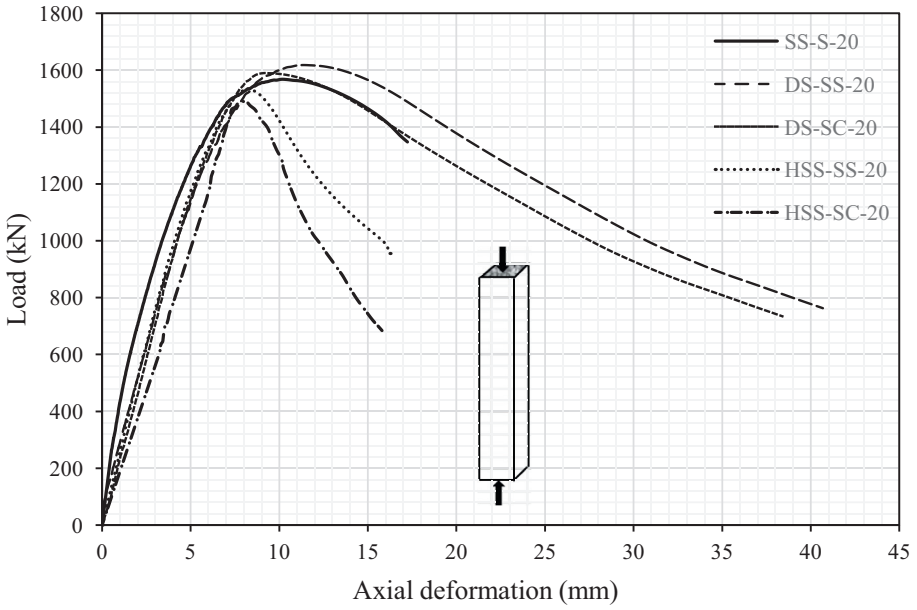

Fig. 7. Axial load verses axial deformation curves.

$$P_{cr} = \frac{\pi^2 EI_{eff}}{L^2} \tag{4}$$

The effective flexural rigidity EI_{eff}, of the cross-section that participates in resisting the elastic buckling of column is computed by linearly adding EI of various components in the cross-section. The EI of sandwiched concrete is reduced by C_3 factor, based on the fact that concrete loses its stiffness due to cracking much before the occurrence of column buckling. Eq. (5) and Eq. (6) are similar to the ones specified for CFST section in AISC-360. The influence of inner steel tube is also considered in quantifying the stiffness degradation of sandwiched concrete (C_3 factor).

$$EI_{eff} = E_{so}I_{so} + E_{si}I_{si} + C_3E_cI_c \tag{5}$$

$$C_3 = 0.6 + 2\left(\frac{A_{so} + A_{si}}{A_{so} + A_{si} + A_c}\right) \leq 0.9 \tag{6}$$

3.2. EC4

The cross-section capacity (P_n) of CFST column as per EC4 is given in Eq. (7), and its modified form for CFDST section is shown in Eq. (8). This capacity equation is also recommended in by Pagoulatou et al. (2014) [22] for CFDST with CHS as inner and outer steel tubes. In square cross-sections, the confinement action within the cross-section is not effective and therefore, enhancement (η_c) and reduction factor (η_s) for concrete and steel strength respectively is specified as zero and unity. It should be noted that in AISC-360, concrete strength is further reduced by 15% for square cross-sections. Also, EC4 does not consider

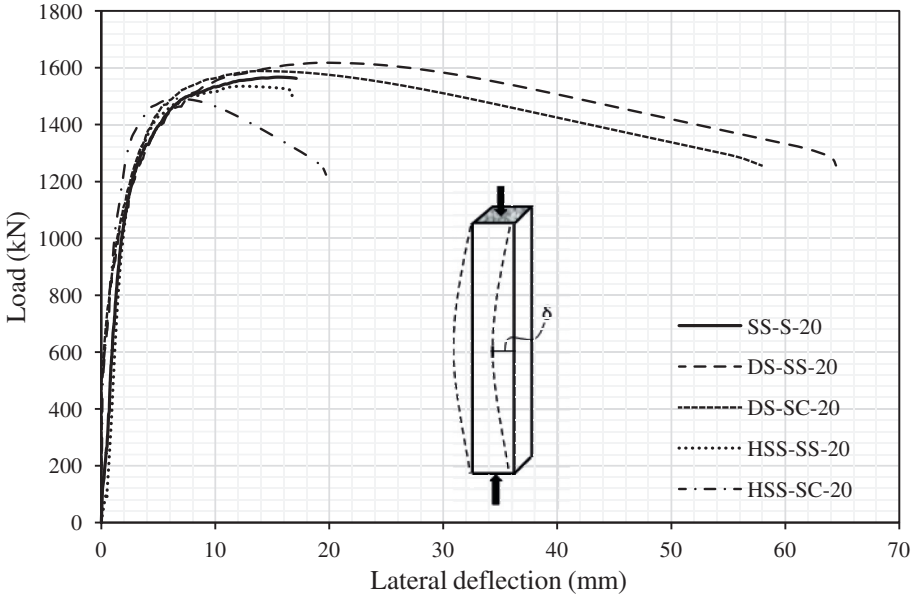

Fig. 8. Axial load verses lateral deflection curves.

Please cite this article as: U. M. S, S. A. J, Axial Compression Behaviour of Long Concrete Filled Double Skinned Steel Tubular Columns, Structures (2016), http://dx.doi.org/10.1016/j.istruc.2016.12.002

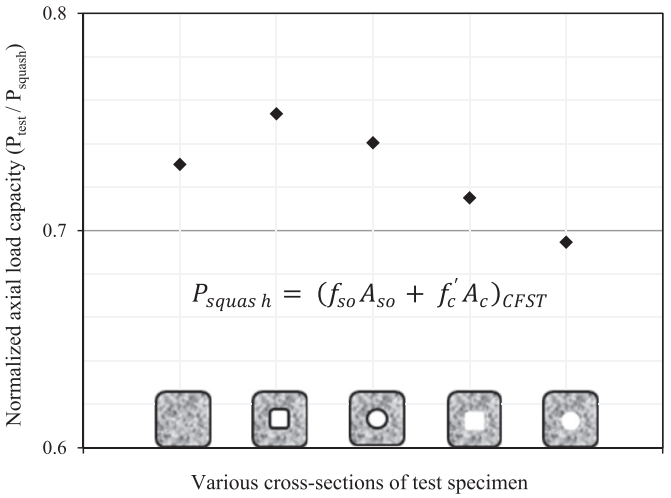

Fig. 9. Normalized axial load capacities of various cross-section of test specimens.

concrete strength enhancement when the slenderness ratio, λ, is >0.5.

$$P_u = \eta_s f_y A_s + \left(1 + \eta_c \frac{t f_y}{D f_c'}\right) f_c' A_c \tag{7}$$

$$P_u = \eta_{so}\left(f_{yo} A_{so} + f_{yi} A_{si}\right) + \left(1 + \eta_c \frac{t_o f_{yo}}{D_o f_c'}\right) \tag{8}$$

$$P_{u,n} = \chi\left(f_{yo} A_{so} + f_{yi} A_{si} + f_c' A_c\right) \tag{9}$$

As classically handled by the codes of practice, the cross-section capacity of long columns is reduced by a stability reduction factor χ, which depends on the slenderness ratio (λ) and imperfection factor (α). The computation of λ is given in Eq. (10), which is a function of cross-section capacity (P_n) and the column elastic buckling load (P_{cr}). The effective flexural rigidity EI_{eff}, is given in Eq. (11). It should be noted that the concrete stiffness reduction in EC4 is much lesser than the one specified in AISC-360.

$$\lambda = \sqrt{\frac{N_u}{P_{cr}}} \tag{10}$$

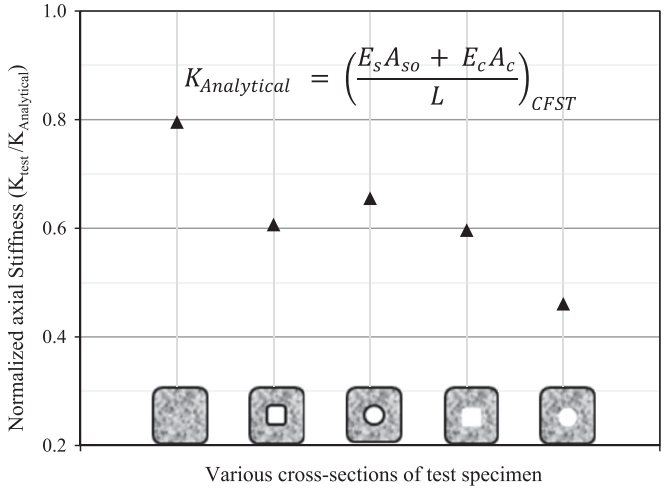

Fig. 10. Normalized axial stiffness of various cross-sections of test specimens.

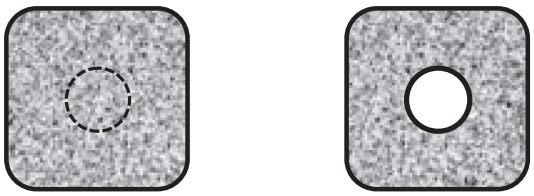

Fig. 11. Formation of CFDST cross-section.

$$EI_{eff} = E_{so} I_{so} + E_{si} I_{si} + 0.6 E_c I_c \tag{11}$$

$$\chi = \frac{1}{\phi + \sqrt{\phi^2 - \lambda^2}} \tag{12}$$

$$\phi = 0.5\left(1 + \alpha\,(\lambda - 0.2) + \lambda^2\right) \tag{13}$$

EC4 considers column imperfection *curve a* for CFST cross-sections. The same trend is adopted for CFDST cross-sections in the present study.

3.3. Han et al. (2009)

The experimental results are also compared with CFDST design formulae proposed by Han et al. (2009). Here, a confinement ratio ξ is introduced which defines and quantifies the confinement action between steel tubes and sandwiched concrete. The proposed cross-section capacity equation is shown in Eqs. (14-a) and (14-b) for circular and square sections respectively.

$$P_n = \left\{C_1\,\chi^2 f_{yo} + C_2\,(1.14 + 1.02\,\xi)\,f_{ck}\right\}(A_{so} + A_c) + A_{si}\,f_{si} \tag{14-a}$$

$$P_n = \left\{C_1\,\chi^2 f_{yo} + C_2\,(1.18 + 0.85\,\xi)\,f_{ck}\right\}(A_{so} + A_c) + A_{si}\,f_{si} \tag{14-b}$$

$$P_{u,n} = \varphi P n \tag{15}$$

$$\varphi = \begin{cases} 1.0 & (\lambda \le \lambda_o), \\ a_1\lambda^2 + b_1\lambda + c_1 & (\lambda_o < \lambda \le \lambda_p), \\ \dfrac{d_1\left(-0.23\chi^2 + 1\right)}{(\lambda + 35)^2} & (\lambda > \lambda_p) \end{cases} \tag{16}$$

Here χ, ξ, φ are hollowness ratio, confinement ratio and stability reduction factor. Coefficients C_1 and C_2 are based on the area of the steel and concrete components within the cross-section. The description of these coefficients is discussed in Han et al. (2009) [12]. The stability reduction factor (φ) for various slenderness ranges is given in Eq. (16).

Table 2a
Comparison of test results with modified capacity equations from EC4 & AISC-360 and Han et al. (2009) [12].

Specimen ID	P_{test} kN	P_{EC4} kN	$P_{AISC-360}$ kN	P_{Han} kN	P_{EC4}/P_{test}	$P_{AISC-360}/P_{test}$	P_{Han}/P_{test}
SS-S-20	1568	1764	1634	1591	1.12	1.04	1.01
DS-SS-20	1618	1860	1752	1729	1.15	1.08	1.07
DS-SC-20	1589	1853	1742	1750	1.17	1.10	1.10
HSS-SS-20	1535	1691	1574	1542	1.10	1.03	1.00
HSS-SC-20	1491	1707	1587	1585	1.14	1.06	1.06
				Mean	1.14	1.06	1.05
				Std dev	0.02	0.03	0.04

3.4. Comparison of test results with analytical predictions

The axial load carrying capacity of specimens from the experimental results is compared with modified EC4 and AISC-360 capacity formulae and also with the design equations proposed by Han et al. (2009) [12], the comparison is presented in Table 2. It is observed that the analytical expressions used are un-conservative in predicting the axial capacity of long column CFDST. The un-conservative error is in the range of 8–10%, using modified AISC-360 equations and 7–10%, using the equations proposed by Han et al. (2009) [12]. The error is highest in the case of modified EC4 equations (in the range of 15–17%).

The analytical expressions are also verified by comparing their results with the experimental study by Romero et al. (2015) [17]. The CFDST sections namely NR1, NR4, NR7 and NR10 are selected from their study for validation. L/D ratio of their specimens is 16.575, t_i, t_o and f_{ck} are the variable parameters within these four cross-sections. Comparison of their test results with the analytical expressions which were framed in the previous section is shown in Table 2b. Analytical results for cross-sections with normal strength concrete (NR1 and NR4) shows high un-conservative error irrespective of the thickness of inner and outer tube. The predictions are found to be slightly conservative in the specimens (NR7 and NR10) with high strength concrete.

The method, in which the stability reduction factor is computed, for the strength predictions of CFDST sections, may not be applicable in reality. This is suspected due to the difference in the yielding behaviour of outer and inner steel tubes, at post-buckling phase. Further, the sandwich concrete cracked while the specimen underwent buckling, and crushed at the regions where the outer steel tube has yielded. Therefore, it is not possible to maintain the composite action between inner and outer steel tubes in this stage of loading. The concept of a single stability reduction factor for the entire cross-section becomes questionable when the strength of the inner steel tube is not fully utilized at the ultimate load point. One way to mitigate this discrepancy is, to introduce a reduction factor in design which can handle the delay in the yield of inner steel tube. Based on this concept, an axial capacity equation is proposed for long column CFDST section with a new reduction factor, presented in Eq. (18). In Eq. (17), χ_1 is the conventional stability reduction factor and χ_2 is the proposed reduction factor to quantify the unutilized strength of inner steel tube at ultimate load point. It is arrived based on strain gradient across the cross-section of CFDST column (Fig. 6). Taking the overall depth of the cross-section h and width of annular ring formed by sandwich concrete a, the reduction incurred in the axial capacity due to the delay in the yielding of inner steel tube of CFDST cross-section is given in Eq. (18). The concrete strength is reduced by 15% for square cross-section as recommended in AISC-360 for CFST columns.

$$P_{u,n} = \chi_1 \chi_2 P_n \tag{17}$$

$$\chi_2 = \frac{1 + \left(1 - \frac{2a}{h}\right)\alpha_s + \alpha_c}{1 + \alpha_s + \alpha_c} \tag{18}$$

Table 2b
Comparison of test results from (Romero et al., 2015) with modified capacity equations from EC4 & AISC-360 and Han et al. (2009) [12].

Specimen ID	P_{test} kN	P_{EC4} kN	$P_{AISC-360}$ kN	P_{Han} kN	P_{EC4}/P_{test}	$P_{AISC-360}/P_{test}$	P_{Han}/P_{test}
NR1	1418	1693	1653	1702	1.19	1.17	1.20
NR4	1644	1940	1875	2132	1.18	1.14	1.30
NR7	2571	2526	2673	2293	0.98	1.04	0.89
NR10	2612	2792	2818	2551	1.07	1.08	0.98
				Mean	1.11	1.11	1.09
				Std dev	0.10	0.06	0.19

Table 3
Comparison of test results with modified capacity equations from EC4 & AISC-360 after incorporating χ_2 factor.

Specimen ID	P_{test} kN	P^a_{EC4} kN	$P^a_{AISC-360}$ kN	P^a_{EC4}/P_{test}	$P^a_{AISC-360}/P_{test}$
DS-SS-20	1618	1636	1624	1.01	1.00
DS-SC-20	1589	1642	1630	1.03	1.03
NR1	1418	1359	1326	0.96	0.94
NR4	1644	1826	1765	1.11	1.07
NR7	2571	2225	2355	0.87	0.92
NR10	2612	2686	2711	1.03	1.04
			Mean	1.00	1.00
			Std dev	0.08	0.06

Here, $\alpha_s = \frac{A_{si} f_{yi}}{A_{so} f_{yo}}$; $\alpha_c = \frac{0.85\, A_c f_c'}{A_{so} f_{yo}}$; $a = \frac{(D_o - 2t_o - D_i)}{2}$; $h = D_o$.

The experimental results in this study and from Romero et al., (2015) [17] are again compared with the proposed axial capacity equation in EC4 and AISC-360 scheme and presented in Table 3. In the proposed equation, the concrete strength is reduced by 15% for square steel tubes in EC4 scheme, owing to its high un-conservative results on comparison with AISC-360 scheme. The proposed equations are more reasonable and they are in good agreement with the experimental capacities of CFDST long columns.

The new reduction factor (χ_2) is applicable only for those column which fails by overall buckling. The range of column length for which the factor has to be incorporated is not distinctly found yet. Also, the influence of thickness ratio of inner and outer steel tubes and concrete strength on χ_2 has to be studied further.

4. Summary and conclusions

Axial compression test is carried out to study the long column behaviour of CFDST. Among the five selected cross-sections, one is CFST (benchmark specimen), two are CFDST, with variation in the inner tube shape and the remaining two are CFHSST. The axial load versus axial deformation curves indicate that the behaviour of all the specimens are similar till the buckling point, later on, in the post-buckling phase, the cross-sections show distinct behaviour owing to the difference in their cross-sectional yielding pattern. The axial load versus lateral deflections are also plotted, and it reverberates the phenomenon which was observed in axial deformation curves. The design procedure of CFST column specified in EC4 and AISC-360 is extended for CFDST by modifying certain parameters. The axial capacity values from these modified code equations and from design formulae proposed by Han et al. (2009) [12] is compared with the experimental results of the present work and Romero et al. (2015) [17]. The analytical results are found to be un-conservative, and inconsideration of the delay in yielding of inner tube is found to be the reason for this error. A new reduction factor is incorporated in the modified AISC-360 and EC4 equations for CFDST column design. The final equation is in good agreement with the test results. The following are some of the conclusions drawn based on this limited research.

- The long column specimens underwent global buckling followed by yielding of the cross-section. On yielding, local bulges are formed in the compression side of outer tube, at the mid-height of the specimen.
- In the initial loading phase (around 80% of ultimate load), all specimen shows linear behaviour till the buckling load point. This is observed in axial load verses axial deformation curves and axial load verses lateral deflection curves. Later, when the specimen started to yield, the behaviour among the specimens varied depending on the type of cross-section.
- Normalized axial capacity and normalized axial stiffness charts were made to compare axial capacity and axial stiffness values of the cross-section considered in this study. The increase in axial capacity

Please cite this article as: U. M. S, S. A. J, Axial Compression Behaviour of Long Concrete Filled Double Skinned Steel Tubular Columns, Structures (2016), http://dx.doi.org/10.1016/j.istruc.2016.12.002

of CFDST section on comparison with corresponding CFHSST section is observed to be marginal. It indicates that the strength of inner steel tube has not been utilized fully at the ultimate load point.
- Delay in the yielding of inner steel tube with respect to the outer steel tube is detected as the reason, in the lesser participation of inner steel tube in axial load resistance of CFDST section.
- A new reduction factor χ_2 is introduced to account the delay in yielding of inner steel tube. This factor is multiplied with modified AISC-360 and modified EC4 equations to find the axial capacity of long column CFDST. The proposed equation is simple, flexible and gives results which are in good agreement with experimental results.

Acknowledgements

The authors are grateful to TATA Steel for sponsoring steel tubes in our experiments. The support from lab staffs of Structural Engineering Laboratory, IIT Madras is also much appreciated.

References

[1] Wright HD, Oduyemi TOS, Evans HR. The design of double skin composite elements. J Constr Steel Res 1991;19:111–32. http://dx.doi.org/10.1016/0143-974X(91)90037-2.
[2] Elchalakani M, Zhao X-L, Grzebieta R. Tests on concrete filled double-skin (CHS outer and SHS inner) composite short columns under axial compression. Thin-Walled Struct 2002;40:415–41. http://dx.doi.org/10.1016/S0263-8231(02)00009-5.
[3] Li W, Ren Q-X, Han L-H, Zhao X-L. Behaviour of tapered concrete-filled double skin steel tubular (CFDST) stub columns. Thin-Walled Struct 2012;57:37–48. http://dx.doi.org/10.1016/j.tws.2012.03.019.
[4] Zhang F, Wu C, Zhao X, Li Z, Heidarpour A, Wang H. Numerical modeling of concrete-filled double-skin steel square tubular columns under blast loading, 29; 2015 1–12. http://dx.doi.org/10.1061/(ASCE)CF.1943-5509.0000749.
[5] Wang R, Han L-H, Zhao X-L, Rasmussen KJR. Experimental behavior of concrete filled double steel tubular (CFDST) members under low velocity drop weight impact. Thin-Walled Struct 2015;97:279–95. http://dx.doi.org/10.1016/j.tws.2015.09.009.
[6] Lu H, Zhao X-L, Han L-HFE. Modelling and fire resistance design of concrete filled double skin tubular columns. J Constr Steel Res 2011;67:1733–48. http://dx.doi.org/10.1016/j.jcsr.2011.04.014.
[7] Hsiao P, Hayashi KK, Nishi R, Lin X, Nakashima M, Asce M. Investigation of concrete-filled double-skin steel tubular columns with ultrahigh-strength steel. J Struct Eng ASCE 2014:1–8. http://dx.doi.org/10.1061/(ASCE)ST.1943-541X.0001126 [ISSN 0733-9445/04014166(8].
[8] Han L-H, Li W, Bjorhovde R. Developments and advanced applications of concrete-filled steel tubular (CFST) structures: members. J Constr Steel Res 2014;100:211–28. http://dx.doi.org/10.1016/j.jcsr.2014.04.016.
[9] Zhao X-L, Grzebieta R. Strength and ductility of concrete filled double skin (SHS inner and SHS outer) tubes. Thin-Walled Struct 2002;40:199–213. http://dx.doi.org/10.1016/S0263-8231(01)00060-X.
[10] Han L-H, Tao Z, Huang H, Zhao X-L. Concrete-filled double skin (SHS outer and CHS inner) steel tubular beam-columns. Thin-Walled Struct 2004;42:1329–55. http://dx.doi.org/10.1016/j.tws.2004.03.017.
[11] Tao Z, Han L-H, Zhao X-L. Behaviour of concrete-filled double skin (CHS inner and CHS outer) steel tubular stub columns and beam-columns. J Constr Steel Res 2004;60:1129–58. http://dx.doi.org/10.1016/j.jcsr.2003.11.008.
[12] Han L-H, Huang H, Zhao X-L. Analytical behaviour of concrete-filled double skin steel tubular (CFDST) beam-columns under cyclic loading. Thin-Walled Struct 2009;47:668–80. http://dx.doi.org/10.1016/j.tws.2008.11.008.
[13] Li W, Han L-H, Ren Q-X, Zhao X-L. Behavior and calculation of tapered CFDST columns under eccentric compression. J Constr Steel Res 2013;83:127–36. http://dx.doi.org/10.1016/j.jcsr.2013.01.010.
[14] Li W, Han L-H, Zhao X-L. Axial strength of concrete-filled double skin steel tubular (CFDST) columns with preload on steel tubes. Thin-Walled Struct 2012;56:9–20. http://dx.doi.org/10.1016/j.tws.2012.03.004.
[15] Essopjee Y, Dundu M. Performance of concrete-filled double-skin circular tubes in compression. Comput Struct 2015;133:1276–83. http://dx.doi.org/10.1016/j.compstruct.2015.08.033.
[16] Romero ML, Espinos A, Portolés JM, Hospitaler A, Ibañez C. Slender double-tube ultra-high strength concrete-filled tubular columns under ambient temperature and fire. Eng Struct 2015;99:536–45. http://dx.doi.org/10.1016/j.engstruct.2015.05.026.
[17] Romero ML, Portolés JM, Espinós A, Pons D, Albero V. Influence of ultra-high strength concrete on circular concrete-filled dual steel columns. Proc 11th Int Conf Adv Steel Concr Compos Struct Tsinghua Univ Beijing, China, December; 2015. p. 161–6.
[18] EN 1994-1-1:2004. Eurocode 4: design of composite steel and concrete structures part 1-1: general rules and rules for buildings. Eur Commun Stand 2004:1–117. http://dx.doi.org/10.1680/dgte4.31517.
[19] Romero ML, Ibañez C, Espinos A, Portolés JM, Hospitaler A. Influence of ultra-high strength concrete on circular concrete-filled dual steel columns. ISTRUC 2016. http://dx.doi.org/10.1016/j.istruc.2016.07.001.
[20] Uenaka K, Kitoh H, Sonoda K. Concrete filled double skin circular stub columns under compression. Thin-Walled Struct 2010;48:19–24. http://dx.doi.org/10.1016/j.tws.2009.08.001.
[21] ANSI/AISC 360-10. Specification for structural steel buildings. Am Inst Steel Constr 2010:1–612 [doi:111].
[22] Pagoulatou M, Sheehan T, Dai XH, Lam D. Finite element analysis on the capacity of circular concrete-filled double-skin steel tubular (CFDST) stub columns. Eng Struct 2014;72:102–12. http://dx.doi.org/10.1016/j.engstruct.2014.04.039.

Please cite this article as: U. M. S, S. A. J, Axial Compression Behaviour of Long Concrete Filled Double Skinned Steel Tubular Columns, Structures (2016), http://dx.doi.org/10.1016/j.istruc.2016.12.002